Eur. Phys. J. D **29**, 357–365 (2004)
DOI: 10.1140/epjd/e2004-00046-x

THE EUROPEAN PHYSICAL JOURNAL D

Rotationally inelastic collisions of electrons with H_2 and N_2 molecules: converged space-frame calculations at low energies

S. Telega[a], E. Bodo, and F.A. Gianturco[b]

Department of Chemistry and INFM, University of Rome "La Sapienza", P.A. Moro 5, 00185 Roma, Italy

Received 18 February 2003 / Received in final form 1st December 2003
Published online 15 April 2004 –

Abstract. The quantum treatment of the collisional excitation of rotations in H_2 and N_2 gases as test molecules is carried out within a space-fixed frame of reference by solving the multichannel close-coupled equations using an approach newly developed in our group, i.e. the modified variable phase approximation (MVPA). The interaction potentials contain the static, exchange and correlation-polarisation contributions and are obtained via a local, multipolar expansion formulation from ab initio data. The results are compared with existing experiments and produce numerically converged rotationally inelastic cross-sections obtained from an exact molecular-frame treatment of the problem.

PACS. 34.80.Bm Elastic scattering of electrons by atoms and molecules – 34.80.Gs Molecular excitation and ionization by electron impact

1 Introduction

It has been known for a long time that electrons penetrating a molecular gas loose a substantial part of their energies by exciting internal degrees of freedom in the gas molecules [1]. A quantity such as the mean energy loss, $\langle \Delta E \rangle$, is therefore, in the case of a diluted gas, the net result of many binary collisions in the gaseous medium which have occurred with molecular targets having different initial internal states and ending up into different final states. It therefore follows that the theoretical determination of $\langle \Delta E \rangle$ for a given ambient gas requires knowledge of the state-to-state cross-sections for many inelastic processes and especially for rotational transitions, since the latter become important consequences of slow impinging electrons being further slowed down from their injection velocities, whereby they can excite electronic and/or vibrational degrees of freedom.

These rotational transitions are of great relevance in the physics of gases and of low-temperature plasmas, for spectral-line broadening, in the relaxation processes within shock-waves and in the thermal balance within the interstellar gas, to cite some of the wide-ranging topics in which they play a significant role [2].

As mentioned before, rotationally inelastic collisions contribute much to electron energy losses only at low energies, where the impinging electron interacts, via the anisotropic potential created by the electronuclear network of the molecular target, with the gaseous molecule and exchanges energy with the latter. Because of the kinematic inefficiency of the process (due to the large mass difference involved) electrons are usually expected to apply a rather small torque to the target molecule and therefore to cause rather small energy transfers at low energies. Furthermore, when the electron energies are larger than, say, 3.0 eV the dynamics deals with rotational times which are long when compared with collisional interaction times [3–5] and therefore suggests that rotationally inelastic cross-sections could be obtained within a simple adiabatic scheme, called the Adiabatic Nuclei Rotations (ANR) [6], whereby only a frame transformation of the Body-Fixed (BF), molecular-frame K-matrix elements yields the final state-to-state rotationally inelastic cross-sections [7]. As the collision energy decreases such an adiabatic decoupling scheme is not really valid and the physics of the events requires the molecular and the projectile angular momenta to be dynamically coupled during the scattering process [8] and through the anisotropic terms of the interaction potential. Furthermore, the existence of strong angular anisotropy features of the potential, the presence of charged partners which extend the range of interaction over a much larger region of space are both difficult elements to handle in order to reach converged results for the ensuing S-matrix multichannel elements (see below for further details).

In the present work we therefore decided to employ full quantum calculations of the rotational excitation processes occurring by electron impact and to use the H_2 and N_2 molecular targets (both in their electronic ground

[a] *Present address*: Faculty of Applied Physics and Mathematics, Technical University of Gdansk, 80952 Gdansk, Poland.
[b] e-mail: fa.gianturco@caspur.it

states) as test examples for which we correctly treat the dynamics in a space-fixed (SF) frame of reference. The state-to-state rotationally inelastic cross-sections are obtained from a full quantum account of angular momenta coupling during the collision and convergence is tested on the final stability of the S-matrix elements.

The following section briefly describes the scattering equations while Section 3 reports the evaluation of the interaction forces. Section 4 presents our results and compares them with some of the experiments for the test systems we have looked at in the present study, while Section 5 gives our conclusions.

2 The quantum dynamics

In this initial test study we shall treat the N_2 and H_2 molecular targets as rigid rotors, disregarding from the time being the effects of vibrational excitations during the rotational energy transfer collisions. Furthermore, since we will focus on rather low-energy collisions, we expect the rotational-to-vibrational mode coupling to be rather inefficient and therefore not to markedly affect pure rotational inelasticity at these energies [9]. Such effects, however, are not in general minor ones, especially at higher collision energies, but will be discussed more in details in future applications. Furthermore, as reported in the following section, the electron interaction with the molecules will be described by a local, energy-dependent effective potential. Here again the non-local nature of the exchange interaction is somewhat simplified in our treatment. However, the present model has already yielded very good results for other, more complicated targets [10] and thus we expect that it will be sufficiently realistic also for the present study.

In the case of the small distortions which are induced into the target rotations by the impinging particle, the total scattering wavefunction can be expanded in terms of asymptotic target rotational eigenfunctions

$$\mathcal{H}_{rot}(\hat{R}_{eq})Y_{jmj}(\hat{R}_{eq}) = \frac{\hbar^2}{2I}j(j+1)Y_{jmj}(\hat{R}_{eq}) \qquad (1)$$

with I being the isolated molecule moment of inertia [11] and $(\hat{R}_{eq})$ the space orientation of the molecular bond, kept at its equilibrium value. Hence, the total scattering wavefunction is given as

$$\Psi_n(E, \mathbf{r}_e, \mathbf{R}_{eq}) = \sum_f u_{i\to f}(\mathbf{r}_e, E)Y_f(\hat{\mathbf{R}}_{eq}) \qquad (2)$$

where $|f\rangle$ denotes the $|j'm_{j'}\rangle$ final states of the rotating molecule that are involved in the expansion and the $u_{i\to f}(\mathbf{r}_e, E)$ are the channel components of the scattering wavefunction which have to be determined by solving the usual Schrödinger equation subject to its scattering boundary conditions, with $\mathbf{r}_e$ being the scattered electron vector position from the molecular center of mass (c.o.m.), with radial component given by

$$u_{i\to f}(r_e) \to \delta_{if}h^{(-)}(r_e) - S_{if}h^{(+)}(r_e) \text{ as } (r_e) \sim \infty \qquad (3)$$

here $h^{(\pm)}(r_e)$ is a pair or linearly independent free partial wave solutions defined as

$$h_{if}^{(\pm)} \sim \delta_{if}k_i^{-1/2}\exp\left[i(k_i r \pm l_i\pi/2)\right]. \qquad (4)$$

When they are chosen to be appropriate Riccati-Hankel functions, then the S_{if} coefficients become the elements of the reduced scattering matrix, often additionally labeled by the total angular momentum of the system: $\mathbf{J} = \mathbf{j} + \mathbf{l}$, the latter $\mathbf{l}$ being the continuum electron partial wave component. Usually, one expects that the numerically converged scattering observables can be obtained by retaining only a limited number of discrete, asymptotic target states in the expansion (2).

The $u_{i\to f}$ are therefore expanded in products of total angular momentum eigenfunctions and of radial functions $\varphi^J_{\lambda\lambda'}(E, r_e)$, where J is the magnitude of the total angular momentum and, $\lambda' = (j', l')$. The radial functions are in turn solutions of the familiar set of coupled, second order homogeneous differential equations (in the case of local interactions) [11,12]

$$\left[\frac{d^2}{dr_e^2}\mathbf{I}^2 - \frac{1}{r_e^2}\mathbf{l}^2 + \mathbf{K}^2\right]\mathbf{\Phi}^J(E, r_e) = \mathbf{U}^J\mathbf{\Phi}^J(E, r_e) \qquad (5)$$

where $\mathbf{I}$ is the unit matrix, $\mathbf{\Phi}^J$ is the matrix of radial functions and atomic units are used throughout this work. Hence

$$(\mathbf{l}^2)_{\lambda\lambda''} = l'(l'+1)\delta_{\lambda'\lambda''} \qquad (6)$$

$$(\mathbf{K}^2)_{\lambda\lambda''} = k^2_{j'}\delta_{\lambda'\lambda''} = 2(E - E_{j'})\delta_{\lambda'\lambda''} \qquad (7)$$

$$(\mathbf{U}^J(r_e))_{\lambda'\lambda''} = 2\sum_L f_L(l'j'; l''j''; J)V_L(r_e) \qquad (8)$$

where the $f_L(l'j'; l''j''; J)$ are the well-known, real coefficients of Percival and Seaton [13] and the coupling between the asymptotic (diabatic) target states is given by the radial matrix elements which we shall discuss in detail in the next section. Since L is even and $f_L(l'j'; l''j''; J)$ is real, the $U^J_{\lambda'\lambda''}$ is nonzero only if $j' - j''$ is even, i.e. the matrix is block diagonal with two subblocks that contain only even values of $(l' + j')$ or only odd values of $(l' + j')$. Thus, when one starts from $j = 0$ it is only necessary to include those values of the partial wave index l for which $|J - j| \le l \le J + j$ and for which $l + J$ is even. When j_{max} is the maximum value of j included in the expansion (2), then the f_L's are zero for $L > 2j_{max}$ when $j' < j_{max}$ and $j < j_{max}$. Thus, the direct coupling between rotational levels will be controlled, as we shall further discuss below, by the largest multipolar coupling V_L included in equation (8).

The number of channels to be included in the expansion for equation (5) obviously depends on the system and on the collision energy. Furthermore, for each selected collision energy it also depends on the region of interaction that is being sampled during the search for the channel eigenfunctions. In the short-range regions, which correspond to the strongest interactions, one should include all those channels which become locally open because of

the attractive features of the given interaction (and which would be asymptotically closed, at least some of them). Their number could be very large in the present situations where the Coulomb interaction diverges over the nuclear cusp regions. On the other hand, in the weaker asymptotic region for $r_e \sim \infty$, only a few of the open channels will be needed. In between these two extreme situations there is a region of interaction, usually quite large for the present ionic forces, where the closed channels change their importance with distance and therefore could be varied in number accordingly. Just to treat such demanding interaction forces during an exact quantum dynamics, we have recently developed [14] a suitable numerical algorithm that judiciously performs such controls along the radial evaluation process and modifies the size of the relevant S-matrix. We have called it the Modified Variable Phase Approximation (MVPA) and have employed it in the present case to solve the set of coupled equations (5). The gain in the computational effort can be of about two orders of magnitude with respect to more conventional methods: the details of the method and on analysis of its performances have been given in reference [14] and will not be repeated here.

Typically, for numerical convergence we needed to use the full coupling from about 10^{-3} Å (the initial integration point) out to 8.0 Å, then we could gradually reduce the K-matrix size out to 600 Å for H_2 and out to 2000 Å for N_2. The total angular momentum values went up to 5 for H_2 and N_2, while the target rotational basis was extended up to 16 for H_2 and up to 28 for N_2. The rotational constant of the former target was taken to be 60.853 cm^{-1}, while it was only 1.98 cm^{-1} for the latter molecule. The multipolar coefficients of the potential expansion went up to $\lambda_{max} = 18$ for the hydrogen target and to $\lambda_{max} = 26$ for the nitrogen target. The corresponding partial wave angular momenta for the scattered electron therefore went up to $l_{max} = 21$ for the H_2 molecule and up to $l_{max} = 33$ for the N_2 molecule. The above parameters produces the level of convergence of the S-matrix elements to be of the order of about 10^{-4}–10^{-5} with respect to further extensions of the CC parameters indicated above. We could therefore consider the present results as being numerically "exact" within the quality of our chosen interaction potential, described in the next section.

3 The electron-molecule interaction

3.1 The single center expansion

Resonant and non-resonant low-energy scattering of electrons from polyatomic targets can be studied theoretically (and computationally) at various levels of sophistication for the description of: (i) the electronuclear structure of the target molecule, (ii) the interaction forces between the bound particles and the impinging electron and (iii) the dynamical formulation of the quantum scattering equations.

We employ an ab initio, parameter-free approach which starts with the target nuclei being kept fixed at their equilibrium geometry, thus disregarding for the moment vibrational excitation processes, which will be discussed in following work. This simplifying scheme goes under the familiar name of Fixed Nuclei (FN) approximation [3] and it strongly reduces the dimensionality of the coupled scattering equations for the dynamics. Furthermore, the target N-electrons in a specific molecular electronic state (which, for the present purpose, is taken to be the ground state) are described using the Hartree-Fock, Self-Consistent Field (SCF) approximation via the Single Determinant (SD) description of its $N/2$ occupied Molecular Orbitals (MOs). In our implementation of the scattering equations the occupied MOs of the targets are again expanded on a set of symmetry-adapted angular functions with their corresponding radial coefficients represented on a numerical grid [15]. In this approach, any arbitrary three-dimensional function describing a given electron, either one of the N bound electrons or the scattering electron, is expanded around a single-center (SCE) usually taken to be the c.o.m. of the global $(N+1)$ electron molecular structure

$$F^{p\mu}(r, \hat{\mathbf{r}}|\mathbf{R}) = \sum_{l,h} r^{-1} f_{lh}^{p\mu}(r|\mathbf{R}) X_{lh}^{p\mu}(\hat{\mathbf{r}}). \qquad (9)$$

The above SCE representation refers here to the μth element of the pth irreducible representation (IR) of the point group of the molecule at the nuclear geometry $\mathbf{R}$. The angular functions $X_{lh}^{p\mu}(\hat{\mathbf{r}})$ are symmetry adapted angular functions given by proper combination of spherical harmonics $Y_{lm}(\hat{\mathbf{r}})$

$$X_{lh}^{p\mu}(\hat{\mathbf{r}}) = \sum_{m} b_{lmh}^{p\mu} Y_{lm}(\hat{\mathbf{r}}). \qquad (10)$$

The details about the computation of the $b_{lmh}^{p\mu}$ have been given by us before and will not be repeated here [15,16].

3.2 The anisotropic potential

For a target which has a closed-shell electronic structure with n_{occ} doubly occupied orbitals φ_i, its interaction with a scattering electron as first given by its Exact Static plus Exchange contributions

$$V_{ESE}(\mathbf{r}) = \sum_{k=1}^{M} \frac{-Z_k}{|\mathbf{r} - \mathbf{R}_k|} + \sum_{i=1}^{n_{occ}} (2\hat{J}_i - \hat{K}_i) \qquad (11)$$

where $\hat{J}_i$ and $\hat{K}_i$ are the usual local static potential and the non-local exchange potential operators, respectively. The index k labels one of the M nuclei located at the coordinate $\mathbf{R}_k$ in the c.o.m., molecular frame of reference (MF). Electron-molecule scattering cross-sections (integral and differential) which are computed using only the V_{ESE} potential show in general limited agreement with experimental data of elastic scattering and become even worse when dealing with resonant scattering. The reason lies in its lack of description of the target response, i.e. of the effects of long-range polarisation of the bound electrons by

the charged projectile and of the short-range dynamical correlation between the latter and the molecular electrons.

At higher collision energies this is reflected in the fact that no electronically inelastic processes can be treated at the ESE level of interaction. At the lower energy, of more direct interest in the present study, the lack of inclusion of the target response leads to the neglect of important polarisation effects which then causes the wrong energy behaviour and magnitude of the elastic cross-sections and which further significantly shifts positions and widths of the shape resonances, if existing. For the case of polyatomic targets we have developed over the years a model, nonempirical treatment of both exchange and correlation forces [15–20] which markedly reduces the computational effort while however producing very good accord with available experimental cross-sections [17,21]. It is that description of the full electron-molecule interaction which we adopt in the present study.

We thus use the Semiclassical Exchange (SMCE) model to treat the bound-continuum exchange interaction [19]. In this model the local momentum of the bound electrons is initially disregarded with respect to that of the impinging one, thereby leading to the neglect of the gradients of the former with respect to the gradient of the latter [19,20]. The details of its derivation have been given extensively in the above references and therefore they will not be repeated here. The final expression of the exchange forces, $V^{SMCE}(\mathbf{r}|k^2)$ is given by an energy-dependent function of the static interaction, V_{ST}, and the target total electron density in terms of its Molecular Orbitals (MO), $\varphi_s(\mathbf{r})$

$$V^{SMCE}(\mathbf{r}|k^2) = \frac{1}{2}\left\{E - V_{ST}(\mathbf{r})\right\} - \frac{1}{2}\left\{[E - V_{ST}(\mathbf{r})]^2 + 8\pi\sum_{s=1}^{N}|\varphi_s(\mathbf{r})|^2\right\}^{1/2} \quad (12)$$

where E is the asymptotic collision energy $E = \frac{1}{2}k^2$ and the index s runs over the occupied MO's of the target. V_{ST} is the statistic interaction with the target electronuclear structure.

To further include in the electron-molecule potential the long-range polarisation terms and the short-range dynamical correlation effects, we have implemented a local energy-independent model potential, $V_{ecp}(\mathbf{r})$, discussed in our earlier work [21]. Briefly, the V_{ecp} potential contains a short-range correlation contribution, V_{corr}, which is smoothly connected to a long-range polarisation contribution, V_{pol}, both terms being specific for electron projectiles. The short-range term is obtained by finding where the two radial coefficients for $l = 0$ first intersect. This has been, in fact, what we found in many cases to be the more effective choice in terms of the global smoothness of the total potential [21]. Hence, one writes down the full potential as

$$V_{ecp}(\mathbf{r}_e) = \begin{cases} V_{corr}(\mathbf{r}_e) & r_e \le r_{match} \\ V_{pol}(\mathbf{r}_e) + \sum_{lm} C_{lm}\, r^{-\lambda}\, Y_{lm}(\hat{\mathbf{r}}_e) & r_e > r_{match} \end{cases} . \quad (13)$$

The C_{lm} coefficients have been determined to make the potential continuous at r_{match} and the exponent λ is a function of l such that: $\lambda(l) = 6, 5, 6$ for $l = 0, 1, 2$ and $\lambda(l) = l + 2$ for $l \ge 3$. The matching functions are chosen in a way in which each term added to V_{pol} after r_{match} has the same functional form of the first term neglected in the perturbation expansion of V_{pol}. The present values of r_{match} for $l = 0$ are around $4.0a_0$ for H_2 and around $5.0a_0$ for N_2. This interaction now corresponds to solving out the scattering equations using Static-Exchange-Correlation-Polarisation (SECP) potentials.

The polarisation term contains the spherical and non-spherical parts of the diatomic dipole polarisabilities:

$$V_{pol}^{(0)} = -\frac{\alpha_0}{2r_e^4}; \text{ and } V_{pol}^{(2)} = -\frac{\alpha_2}{2r_e^4}P_2(\cos\hat{\mathbf{r}}_e \cdot \hat{\mathbf{R}}_{eq}) \quad (14)$$

for the $H_2(R_{eq})$ the α_0 value was $5.43a_0^3$, while it was $11.80a_0^3$ for $N_2(R_{eq})$; correspondingly, the two α_2 values were, respectively $1.32a_0^3$ and $3.08a_0^3$. The full SECP interaction was then rewritten using the familiar multipolar expansion in the Space-Frame (SF) reference system of its Jacobi coordinates

$$V_{SECP}(\mathbf{r}_{e'}|\mathbf{R}_{eq}) = \sum_{L=0,\ even}^{L_{max}} V_L^{SECP}(r_e)P_L(\cos\ \hat{\mathbf{r}}_e \cdot \hat{\mathbf{R}}_{eq}). \quad (15)$$

The individual multipolar coefficients were then fitted with spline functions and the expansions extended up to the L_{max} values for H_2 and N_2 already mentioned in Section 2. A pictorial example of the lowest multipolar coefficients ($L = 0$) for both molecules is shown in Figure 1, where one clearly sees the longer range of action of the full potential in the case of N_2 with respect to H_2.

4 The computed cross-sections

4.1 Results for the H_2 molecular target

As discussed in the introduction, the colliding electron and molecule exchange only a small amount of angular momentum quanta. Therefore, for homonuclear molecules only transitions $j \to j$ or $j \to j \pm 2$ and $j \pm 4$ are important. The usual adiabatic approximation invoked to evaluate such transitions [22], as mentioned earlier, allows one to extract approximate values by exploiting the well-known impulse conditions (e.g. see: [23])

$$\left(\frac{k_j}{k_{j'}}\right) d\sigma(j \to j')/d\Omega = \sum_{J \ge \Delta j} \left\{C(jJj';000)\right\}^2 (k_0/k_j) \times d\sigma(0 \to J)/d\Omega. \quad (16)$$

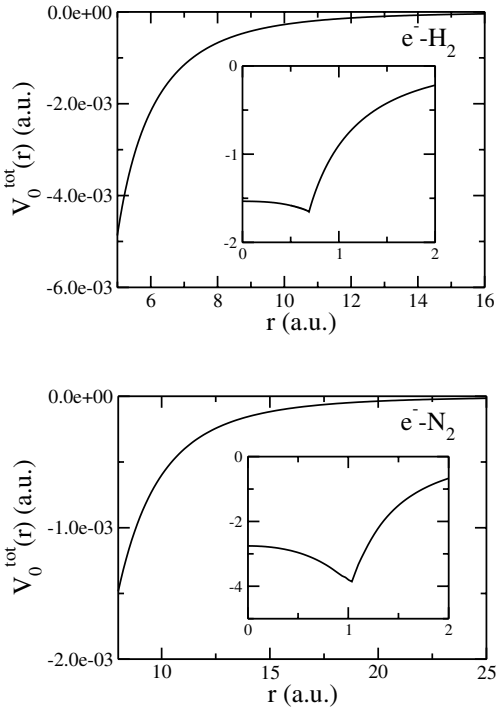

Fig. 1. Radial behaviour of the spherical components for the computed e^--molecule potentials. Upper panel: H_2, lower panel: N_2.

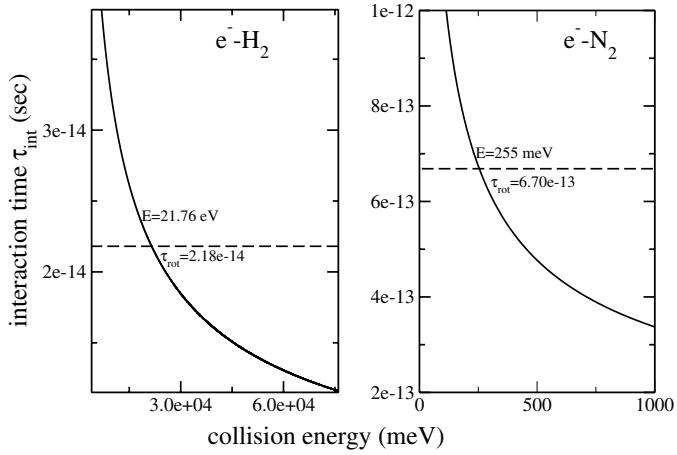

Fig. 2. Computed interaction times as a function of collision energies. The dashed lines show the values of the rotational times, τ_{rot}, for the $(0 \rightarrow 2)$ transitions for H_2 and N_2 treated as rigid rotors.

The above relation has therefore been used extensively in the past to extract estimates of the inelastic/elastic, state-to-state cross-sections from low-energy swarm data [24]. The SF coupling scheme becomes mandatory for rotationally inelastic collisions where the molecular rotational time, τ_{rot}, is shorter than the e^--molecule interaction time, τ_{int}. Figure 2 shows the behaviour of such quantities for the present targets and clearly indicates the boundaries. The exact computational approach thus treats the quantum energy transfer process more correctly and rigorously by carrying out the dynamical coupling between

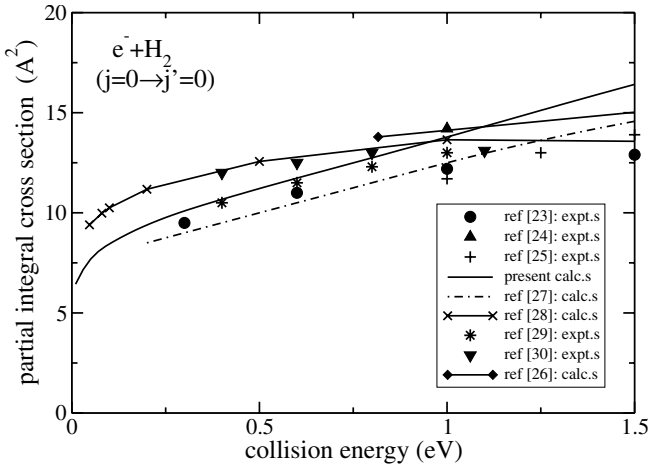

Fig. 3. Computed and measured elastic partial integral cross-sections for $e^- - H_2$ collisions. The solid line reports present calculations while the other curves report earlier experiments and calculations. See inset for the explicit references.

the molecular rotational states and the potential torque applied by the anisotropic force field induced by the impinging electron during the encounter and should solve the scattering equations on the correct energy shell. The use of accurate dynamical treatments for rotationally inelastic cross-section calculations is expected to play a significant role at low collision energies, where the sudden scheme implied by equation (15) is no longer valid. We therefore limit our present study to that energy range where our space-frame rotational close coupling (SF-RCC) treatment should be preferred.

The study of such quantities has a long history for the H_2 molecule [22–34] but the calculations which have been carried out usually employed simplified models to generate the lower multipolar coefficients of equation (15) [26–28] while in the present study we have employed the "exact" static interaction, the correct dipole polarisabilities in the long-range region and we used a non-empirical, local modelling of exchange and correlation forces which has produced before very good accord with the available experimental observables for more complicated molecular targets [15–18].

In the SF-RCC calculation we used a step size of 10^{-3} Å starting near the center-of-mass origin and extending the integration out to 600 Å, switching to the variable phase integrator beyond about 8 Å, as discussed before. The multipolar expansion of equation (15) was kept till $L_{max} = 18$ while 9 rotational states ($j_{max} = 16$) where included in the set of the SF-RCC equations. The higher partial wave value went to $l_{max} = 21$, with about 600 coupled equations per symmetry. The rotational constant was taken as 60.853 cm^{-1}. We therefore claim that the present cross-sections are numerically converged to within 10^{-3} of their values. In other words, within the accuracy of the interaction forces the coupled-channel results are essentially exact.

The results reported in Figure 3 show our low-energy computed integral cross-sections for the $\sigma(j = 0 \rightarrow j = 0)$

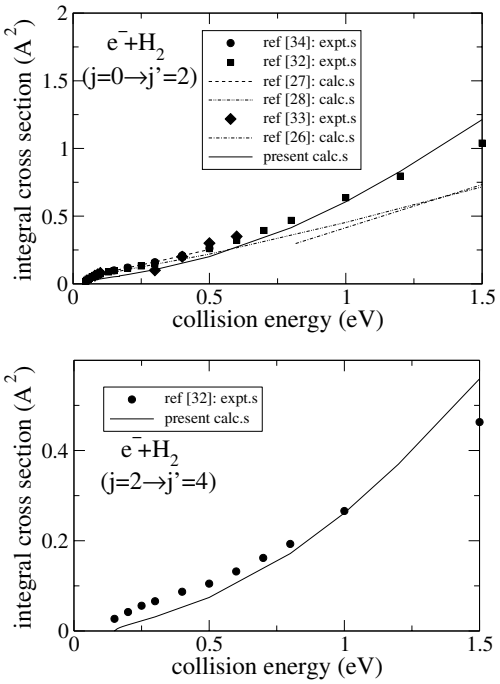

Fig. 4. Same as in Figure 3 but for the inelastic collisions. Upper panel: ($j = 0 \rightarrow j' = 2$) excitations. The solid line shows present calculations while the experiments and the other calculations are labeled as described in the inset. Lower panel: ($j = 2 \rightarrow j' = 4$) excitations. The notation is the same as that of the upper panel.

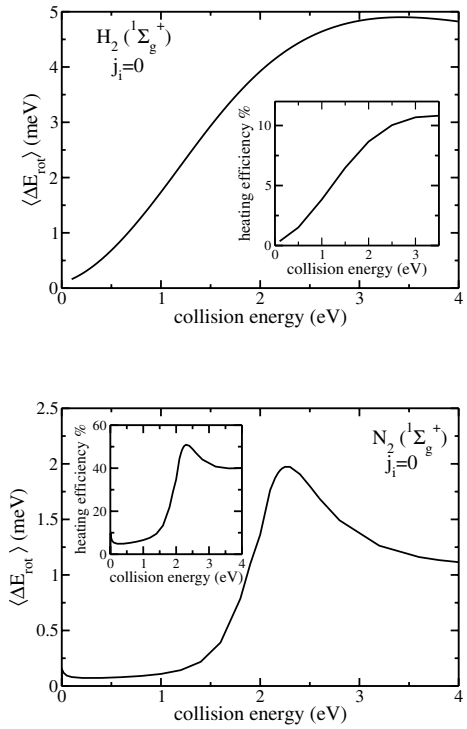

Fig. 5. Computed efficiency indicators for the rotational excitation processes by electron impact at low energy for the H_2 and N_2 molecules, upper and lower panel respectively. The two panels report the average energy transfers as defined by equation (17) while the two insets show the heating efficiency values, C_{he}, from equation (18).

process. The "experimental" data given by the filled-in symbols in the same figure were extracted from swarms data using equation (16) as discussed before: they were reported by Shimamura in reference [23] and by others in references [24,25], with the earlier data given in references [29,30]. The low energy behaviour is shown up to 1.5 eV and indicates the good accord that our calculations attain in that energy region where swarms data achieve the highest reliability. The references for the experimental data are given in the figure. We also report earlier theoretical calculations [26–28] which used approximate interaction potentials and obtained the cross-sections either in an SF frame [26,27] or from the adiabatic transformation [28]: our present results remain fairly close to experiments in comparison with the other calculations.

The inelastic cross-sections for the ($0 \rightarrow 2$) and the ($2 \rightarrow 4$) excitations are shown, again for the same low-energy region, in Figure 4, upper and lower panels respectively. The measurements reported are from reference [33] and were extracted from measured swarms data [32,34]. The dotted curves are calculations from reference [28] while the dot-dashed curves are calculations from reference [26] and the dashed curve reports calculations from reference [27]. Here again one sees that the present approach yields cross-sections which are fairly close to the experimental quantities and follows measurements the closest beyond a collision energy of about 0.75 eV. The calculations of reference [28], dotted curve are also reported: one sees that those calculations, at very low energies, are closer to the swarms data than the present calculations while, at higher energies, the agreement worsens and the present, model interaction produces inelastic cross-sections closer to experiments.

Other quantities of interest for obtaining the excitation efficiency of electron beams in diluted molecular gases could be obtained by evaluating the average energy transfer, $\langle \Delta E \rangle_{rot}$, out of the lowest rotational level of H_2, $j = 0$

$$\langle \Delta E \rangle_{tot}(j=0) = \frac{\sum_{j'} \Delta\varepsilon_{jj'} \sigma(j \rightarrow j')}{\sum_{j'} \sigma(j \rightarrow j')} \qquad (17)$$

and also by computing the so-called heating efficiency coefficient, C_{he}, given as

$$C_{he} = \frac{\sum_{j' \neq j} \sigma(j \rightarrow j')}{\sum_{j'} \sigma(j \rightarrow j')} \qquad (18)$$

which describes the relative flux going into the excited rotational states of the molecule (starting from its ground state) due to the inelastic collisions.

The low-energy behaviour of such quantities for the H_2 molecule is shown in the top panel of Figure 5, where the C_{he} coefficient is reported in the inset of that figure. One clearly sees there that for a light molecule like H_2, with very large energy spacing between rotational levels and with very high rotational speeds in the classical sense, the excitation by low-energy electron is not an efficient process, although it reaches its largest values in the

energy region where a broad shape resonance is thought to occur during the collision process [24]. On the whole, however, the efficiency of the rotational energy transfer in this system does not go beyond about 12% of the total available flux.

4.2 Rotational excitation of N_2 molecules

Both the theoretical and experimental studies on the rotational excitation of N_2 by collision with electrons have been studied frequently over the years, although the number of direct experimental tests has been fairly limited. For instance, their experimental determination from beam data at energies around the resonance structure was performed a while ago [36] and further data at lower energies were produced a little later [37]. Combined experimental and theoretical studies were published later on, in relation to near-threshold swarms data and in the presence of vibrationally inelastic processes [34,37,38]. Pure rotationally inelastic cross-sections at very low energies have been computed in the 80's [38–41] and in even earlier model calculations [42–45]. The latter results were all obtained at higher energies beyond the resonant structure and all confirmed the realistic description of exchange forces through the SCE model potential as we have described earlier and which we have used in the present work.

In the evaluation of the potential multipolar coefficients the L values went up to $L_{max} = 26$, using the experimental dipole polarisability of N_2. The number of rotational levels went up to $j_{max} = 28$ and the radial integration was extended out to 2000 Å, with a variable step size that started at 10^{-3} Å near the potential origin. The rotational constant of the molecule is much smaller than in the case of H_2: 1.985 cm^{-1}. The highest value of the scattered partial wave therefore was $l_{max} = 28$, providing sets of coupled equations, for each even and odd symmetry, of about 1,800 equations. We report in Figure 6 the available experimental data, the earlier calculations and our present results. The values refer to the partial integral cross-sections for the elastic ($j = 0 \rightarrow j = 0$) process.

The experimental data, listed by the captions in the figure, correspond to the beam measurements of Jung et al. (filled circles) from reference [36], to the low-energy data of Sun et al. (filled diamonds) from reference [38], and to further beam data at lower energies by Sohn et al. (filled squares) from reference [37]. The dashed-dotted line gives the calculated values of reference [28], while those of reference [40], that include a parametrisation of the resonant structures to reproduce the oscillations seen experimentally are given by the dotted line. Our own results are shown by the solid line. The dashed line gives the results of the calculations from [41]. The following considerations could be made at this point:

1. the present SF dynamics calculations turn out to come fairly close to the experiments available, all the way from the very-low energy range and through the resonance region, while some of the calculations (i.e. those given by the dotted line and the dot-dashed line) fail in the resonance region;

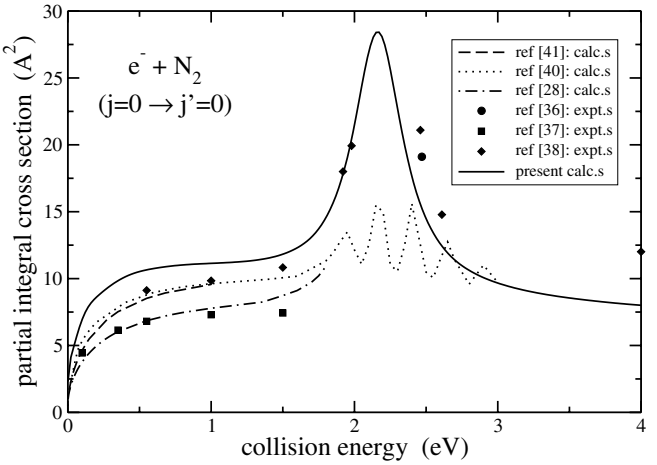

Fig. 6. Computed and measured rotationally elastic partial integral cross-sections for the N_2 molecule. The solid line shows present results while the earlier calculations and experiments also reported are labeled as given in the inset.

2. it is also reassuring to see that also the width of the resonance is well reproduced by the present results: they follow very closely the data of Jung [36] and Sun [38]. Naturally, as no vibrational coupling is included in our calculations, no vibrational structure is present across the resonance region in our computed cross-sections.

The rotationally inelastic, partial cross-sections for the $\sigma(j = 0 \rightarrow j' = 2)$ and $\sigma(j = 0 \rightarrow j' = 4)$ are reported in Figure 7. The filled-in diamonds refer to the fitted swarms data using a low-energy modelling with dominant quadrupole term, as discussed in reference [34]. Their fitting that further includes polarisation contributions is given by the dash-dash-dot curve [34]. The earlier calculations by Onda [40] are shown by the dotted line: they employed a modelled interaction potential with a parametric factor that adjusted its value over the vibrational resonances to reproduce the experimental oscillations. The calculations from reference [45] are given by the dash-dotted line. We also report the calculations of reference [41], given by the chained curve, as indicated in the figure. The present computation, carried out in the SF frame (solid line), is able to go down to very low collision energies and to well represent the cross-section threshold behaviour as it is provided by the modified effective range theory (MERT) employed earlier [41]. On the whole, however, calculations are all over the place and the lack of reliable, direct experiments on the excitation process in this molecule prevents us from selecting the most reliable computed results among those available.

The corresponding inelastic cross-sections for the ($j = 0 \rightarrow j = 4$) excitation process are also reported in Figure 7, lower panel. We also report the calculations from reference [41] (broken line) and those from a private communication by Morrison [39] (chain curve). The estimated threshold behaviour from the swarms data [34], reported by the dot-dashed line, is seen in the inset and is very well reproduced by our calculations (solid line). In contrast to this, the calculations from reference [40] (dotted

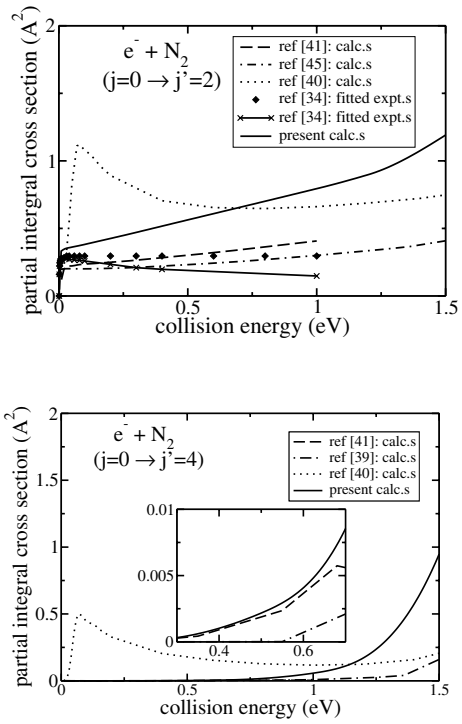

Fig. 7. Same as in Figure 6 but for the rotationally inelastic partial integral cross-sections ($j = 0 \rightarrow j' = 2$), upper panel, and ($j = 0 \rightarrow j' = 4$), lower panel. The present calculations are given by the solid line. Other calculations and the fitted experiments are reported as described by the insets in both panels.

line) show a spurious peak at threshold. The calculations from references [39,41] are also shown and agree with the present data at very low energies (see inset).

The same efficiency indicators are given in Figure 5 for the N_2 molecular target. The calculations indicate clearly that the excitation efficiency increases dramatically within the energy region of the shape resonance: the lengthened interaction time in fact, allows the impinging electron to transfer energy more effectively into molecular rotations. We therefore see from that figure than in the energy range between about 1.5 and 2.3 eV the average energy transfer rises from about 2.0 meV up to about 15 meV, i.e. it increases by at least an order of magnitude. The same effect appears to occur for the C_{he} parameter: around the resonant energy it becomes more than 50%, clearly larger than in the case of the H_2 molecule, where it does not go above 12% of the total flux. The smaller rotational constant of the N_2 molecule, as well as the markedly stronger anisotropy of the $e^- - N_2$ interaction, therefore plays here a significant role in allowing the electron to apply larger torques to molecular rotations during collisional events.

5 Present conclusions

In this work we have undertaken to implement a newly proposed integration scheme for ionic interaction, the MVPA method [12] for e^--molecule collisions at low energy and to analyse with it numerically converged rotational excitation cross-sections of H_2 and N_2 at low energies down to their threshold openings, employing a parameter-free model interaction. In order to reach numerical convergence we have treated the quantum dynamics within a space frame (SF) reference instead of employing the more conventional Body-Fixed (BF) frame of reference (e.g. see Ref. [3]). The electron-molecule interaction was constructed from ab initio model calculations for two fairly well studied diatomic targets like H_2 and N_2 [1]. Our approach is, however, totally general and we are currently extending the code to treat spherical and nonspherical rotors to handle nonlinear polyatomics [46]. The numerical convergence of the S-matrix elements was checked to be around $10^{-4} - 10^{-5}$ and the computational savings of the present method is about two orders of magnitude with respect to earlier propagators [12].

The results clearly show, for both systems, that the exact SF treatment of the dynamics allows us to obtain realistic estimates of elastic and inelastic rotational cross-sections, down to very small collision energies, even when using model potentials. The comparison with available measurements shows at times rather good agreement for both molecules, for which our present computational tools makes it somewhat easier to obtain numerically converged coupled-channel results.

The present calculations further show, as expected, that rotationally inelastic transitions induced by electron impact, albeit occurring in general with low efficiency, become much more probable when taking place in the presence of strong narrow resonances (like in the case of N_2) and to also increase in size with the increase of density of states of the target rotational manifolds. The actual numerical values of the calculated cross-sections could be obtained on request from the authors.

One of us (S.T.) thanks the Erasmus program for supporting part of his stay in Rome while this work was carried out. F.A.G. thanks the Max-Planck Society for a Research Prize Award during the development of the present study and for its support to S.T. during a further visit to Rome. All authors are grateful to the Italian Ministry for University and Research (MUIR) for financial support and to Prof. Jozef Sienkiewicz for his help and support in establishing the Rome-Gdansk collaboration though the Erasmus program. Finally, we are grateful to professor Morrison for his kind help and advice, especially for sending us his unpublished calculations on H_2 and N_2. S.T. also wishes to thank A. Grandi for his help and patience on the use of the VOLLOC scattering code.

References

1. For a recent review see: M.J. Brunger, S.J. Buckman, Phys. Rep. **357**, 215 (2002) and references quoted therein
2. For a summary see: *Swarm Studies and Inelastic Electron-Molecule Scattering*, edited by L.C. Pitchford, V. Mc Koy, A. Chutjian, S. Trajmar (Springer-Verlag, Berlin, 1986)
3. E.S. Chang, A. Temkin, Phys. Rev. Lett. **23**, 399 (1969)
4. S.I.K. Chu, A. Dalgarno, Proc. Roy. Soc. A **345**, 191 (1975)

5. U. Fano, D. Dill, Phys. Rev. A **6**, 185 (1972)
6. D.M. Chase, Phys. Rev. **104**, 838 (1956)
7. K. Takayanagi, Y. Itikawa, Adv. At. Mol. Phys. **6**, 105 (1970)
8. E.S. Chang, U. Fano, Phys. Rev. A **6**, 173 (1972)
9. E.g. see: M.A. Morrison, W. Sun, in *Computational Methods for electron-Molecule Collisions*, edited by W.M. Huo, F.A. Gianturco (Plenum Publ. Press, New York, 1995)
10. E.g. see: F.A. Gianturco, A. Jain, Phys. Rev. **143**, 347 (1986)
11. E.g. see: F.A. Gianturco, *The Transfer of molecular energies by collision* (Springer-Verlag, Berlin, Heidelberg, New York, 1979)
12. W. Eastes, D. Secrest, J. Chem. Phys. **56**, 640 (1972)
13. I.C. Percival, M.J. Seaton, Proc. Comb. Phil. Soc. **53**, 654 (1957)
14. R. Martinazzo, E. Bodo, F.A. Gianturco, Comp. Phys. Comm. **151**, 187 (2003)
15. F.A. Gianturco, R.R. Lucchese, N. Sanna, J. Chem. Phys. **100**, 6464 (1994)
16. E.g. see: R. Curik, F.A. Gianturco, N. Sanna, Int. J. Quantum Chem. **84**, 565 (2001)
17. R. Curik, F.A. Gianturco, J. Phys. B **35**, 1235 (2002)
18. F.A. Gianturco, Yu. Kashenock, R.R. Lucchese, N. Sanna, J. Chem. Phys. **116**, 2811 (2002)
19. F.A. Gianturco, S. Scialla, J. Phys. B **20**, 3171 (1987)
20. F.A. Gianturco, S. Scialla, J. Chem. Phys. **87**, 6468 (1987)
21. F.A. Gianturco, J.A. Rodriguez-Ruiz, A. Jain, Phys. Rev. A **48**, 4321 (1993)
22. I. Shimamura, J. Phys. B **15**, 93 (1982)
23. I. Shimamura, Sci. Papers. Inst. Phys. Chem. Res. **82**, 1 (1989)
24. J. Furst, M. Maghere fteh, D.A. Golden, Phys. Rev. A **30**, 2256 (1984)
25. M.J. Brunger, S.J. Buckman, D.S. Newman, D.T. Alle, J. Phys. B **24**, 1435 (1991)
26. N.F. Lane, S. Geltman, Phys. Rev. **145**, 160 (1957)
27. R.J. Henry, N.F. Lane, Phys. Rev. **183**, 221 (1969)
28. M.A. Morrison, A.N. Feldt, D. Austin, Phys. Rev. A **29**, 2518 (1984)
29. E. Golden, H.W. Bandel, J.A. Salerno, Phys. Rev. **146**, 40 (1966)
30. C. Ramsauer, R. Kollath, Ann. Phys. **4**, 91 (1929)
31. N.F. Lane, S. Geltman, Phys. Rev. **184**, 46 (1969)
32. A.G. Engelhard, L.P. Elford, R.W. Crompton, J. Phys. B **61**, 573 (1988)
33. A.G. Engelhard, A.V. Phelps, Phys. Rev. **131**, 2115 (1963)
34. A.G. Robertson, M.T. Elford, R.W. Crompton, M.A. Morrison, W. Sun, W.K. Trail, Aust. J. Phys. **50**, 441 (1997)
35. E.g. see: *Electron-Molecule Interactions and their applications*, edited by L.G. Christophorou (Academic Press, New York, 1984), Vol. I
36. K. Jung, Th. Antoni, R. Müller, K.H. Kochem, H. Ehrhardt, J. Phys. B **15**, 3535 (1982)
37. W. Sohn, K.H. Kochem, K.-M. Schewerlein, K. Jung, H. Ehrhardt, J. Phys. B **19**, 4017 (1988)
38. W. Sun, M.A. Morrison, W.A. Isaacs, W.K. Trail, D.T. Alle, R.J. Gulley, H.J. Brennan, S.J. Buckman, Phys. Rev. A **52**, 1229 (1995)
39. M.A. Morrison, private communication
40. K. Onda, J. Phys. Soc. Jpn **54**, 4544 (1985)
41. M.A. Morrison, B.C. Saha, T.L. Gibson, Phys. Rev. A **36**, 3682 (1987)
42. M.A. Brandt, D.G. Truhlar, F.A. Van-Catledge, J. Chem. Phys. **64**, 4957 (1979)
43. K. Onda, D.G. Truhlar, J. Chem. Phys. **71**, 5107 (1979)
44. L.A. Collins, W.D. Robb, M.A. Morrison, J. Phys. B **11**, L777 (1978)
45. M.A. Morrison, W. Sun, W.A. Isaacs, W.K. Trail, Phys. Rev. A **55**, 2786 (1997)
46. E. Bodo, F.A. Gianturco, in preparation